

Static and dynamic cultivation of bone marrow stromal cells on biphasic calcium phosphate scaffolds derived from an indirect rapid prototyping technique

M. Schumacher · F. Uhl · R. Detsch ·
U. Deisinger · G. Ziegler

Received: 10 May 2010 / Accepted: 24 August 2010 / Published online: 21 September 2010
© Springer Science+Business Media, LLC 2010

Abstract The adequate regeneration of large bone defects is still a major problem in orthopaedic surgery. Synthetic bone substitute materials have to be biocompatible, biodegradable, osteoconductive and processable into macroporous scaffolds tailored to the patient specific defect. Hydroxyapatite (HA) and tricalcium phosphate (TCP) as well as mixtures of both phases, biphasic calcium phosphate ceramics (BCP), meet all these requirements and are considered to be optimal synthetic bone substitute materials. Rapid prototyping (RP) can be applied to manufacture scaffolds, meeting the criteria required to ensure bone ingrowth such as high porosity and defined pore characteristics. Such scaffolds can be used for bone tissue engineering (BTE), a concept based on the cultivation of osteogenic cells on osteoconductive scaffolds. In this study, scaffolds with interconnecting macroporosity were manufactured from HA, TCP and BCP (60 wt% HA) using an indirect rapid prototyping technique involving wax ink-jet printing. ST-2 bone marrow stromal cells (BMSCs) were seeded onto the scaffolds and cultivated for 17 days under either static or dynamic culture conditions and osteogenic stimulation.

While cell number within the scaffold pore system decreased in case of static conditions, dynamic cultivation allowed homogeneous cell growth even within deep pores of large (1,440 mm³) scaffolds. Osteogenic cell differentiation was most advanced on BCP scaffolds in both culture systems, while cells cultured under perfusion conditions were generally more differentiated after 17 days. Therefore, scaffolds manufactured from BCP ceramic and seeded with BMSCs using a dynamic culture system are the method of choice for bone tissue engineering.

1 Introduction

While autografting remains the standard therapy for critical size bone defects, several synthetic bone substitute materials have been investigated and developed over the last decades to overcome the drawbacks of autologous bone transplantation such as cost, patient pain and limited availability [1]. Gazdag et al. defined the following requirements for an optimal graft material: a three dimensional, porous, osteoconductive matrix that allows ingrowth of bone progenitor cells and vascularisation (I), osteoinductive factors that recruit progenitor cells from the host tissue and induce bone formation (II), graft cells capable of differentiating into osteoblasts (III) and mechanical strength to ensure tissue integrity until the bone healing process is completed (IV) [2, 3].

Synthetic bone graft materials used today include metals, polymers, ceramics and polymer/ceramic-composites. Calcium phosphate (CaP) ceramics, that are available in various forms like porous blocks, granules or mouldable cements, have been given special focus due to their excellent biocompatibility [1, 2, 4]. However, the use of synthetic bone grafts only meets the criteria I and IV

M. Schumacher (✉) · U. Deisinger · G. Ziegler
Friedrich-Baur-Research Institute for Biomaterials,
University of Bayreuth, 95440 Bayreuth, Germany
e-mail: matthias.schumacher@fbi-biomaterialien.de

U. Deisinger
e-mail: ulrike.deisinger@fbi-biomaterialien.de

G. Ziegler
e-mail: guenter.ziegler@fbi-biomaterialien.de

F. Uhl · R. Detsch · G. Ziegler
BioCer Entwicklungs-GmbH, 95447 Bayreuth, Germany
e-mail: franziska.uhl@biocer-gmbh.de

R. Detsch
e-mail: rainer.detsch@biocer-gmbh.de

mentioned above. Hence, the concept of bone tissue engineering (BTE) was introduced, involving the preoperative seeding of the scaffold with cells and/or loading with proteins (e.g. growth factors or cytokines) in order to improve the regenerative potential of the bone graft. The scaffold acts as a template to preserve tissue volume and shape, as a source of growth factors and graft cells (criteria II and III) and is replaced by native tissue over time [4, 5].

Bone marrow stromal cells (BMSCs) are progenitor cells of the skeletal tissue. During bone generation BMSCs proliferate, differentiate into osteoblastic precursor cells and finally into osteoblasts that form extracellular matrix which in turn undergoes mineralisation. These processes are characterised by the expression of specific markers like collagen I and transforming growth factor β (TGF- β), alkaline phosphatase (ALP) and finally bone sialoprotein (BSP), osteopontin (OP) and osteocalcin (OC), respectively [6].

In BTE, these cells are seeded and cultivated on scaffolds to establish a bone-like living tissue. The osteoblastic differentiation is stimulated by the scaffolds' chemistry and morphology as well as the supply of nutrients, growth factors and, if applicable, mechanical stimulation [7]. Since BMSCs can relatively easily be harvested from bone marrow, the patient's own osteoblastic precursor cells may be used, avoiding immunological as well as ethic concerns related to allogenic cells [1].

Calcium phosphate (CaP) ceramics such as hydroxyapatite (HA) and tricalcium phosphate (TCP) are considered as the most suitable ceramic materials for bone reconstruction and BTE since they are highly biocompatible and osteoconductive [8]. CaP ceramics can be degradable and, furthermore, their mechanical strength is sufficient for bone reconstruction in non load-bearing applications [8–10]. The characteristics of biphasic calcium phosphate (BCP) ceramics are based on the balance between the more soluble tricalcium phosphate and the less soluble hydroxyapatite. By varying the HA/TCP ratio, the mechanical and biological performance of the ceramic can be tailored [11–13].

Besides material composition, an important characteristic of scaffolds that shall promote tissue ingrowth and new bone formation is their macrostructure. Cell migration and tissue penetration into the scaffold require a minimum pore size of 50–100 μm , an optimal ingrowth of osteoblast cells requires pore sizes of 200–400 μm [14, 15]. For vascularisation a pore size of even >300 μm is recommended [16]. In general, an open porosity above 50 vol% and pore sizes in the range of 200–800 μm are considered as optimal for bone tissue ingrowth [9, 16–19].

Numerous techniques have been employed in the last years to manufacture ceramic bone implants and bone tissue engineering scaffolds meeting these requirements,

including rapid prototyping (RP). Due to their layer-by-layer approach, RP techniques offer the possibility to fabricate individually adapted scaffolds with high accuracy and few design limitations directly from the desired material [20]. Another concept employs RP methods to fabricate a negative mould that is subsequently used to shape a castable material (indirect RP), making it possible to process also materials not suitable for direct RP. Thus, wax ink-jet printing has been applied to manufacture moulds for porous CaP ceramic scaffolds as well as ceramic/polymer-composites with pores ranging from 150 to 2,000 μm diameter [21–23] to be used as bone substitute. Such scaffolds have been cultivated with various cell types to study cell differentiation and the development of bone tissue. Our group has shown that scaffolds fabricated via this technique lead to higher differentiation of bone marrow stromal cells compared to scaffolds produced by another RP technique, dispense-plotting [24]. Other authors demonstrated *in vitro* cell growth as well as *in vivo* tissue penetration and ectopic bone formation within wax ink-jet printing derived HA scaffolds pre-seeded with bone marrow stromal cells [25]. However, cultivation of cells within large, porous scaffolds comprises the problem of ensuring an appropriate oxygen and nutrient supply which may not be maintained by diffusion processes alone [26]. Therefore, various bioreactor systems have been developed in order to overcome these limitations. Spinner flasks, rotating vessels and perfusion bioreactors are widely used [27]. All these reactor systems have in common that scaffolds are perfused with culture medium while the flow conditions range from defined laminar to undefined turbulent flow. Particularly, the stimulatory effect of the specific bioreactor system on the cells is an important aspect. Perfusion of the scaffolds leads to shear stresses that can either stimulate or inhibit cell proliferation and differentiation. Bancroft et al. have shown that cell differentiation could be accelerated with increasing flow rate (from 0.3 to 3 ml/min) [28]. However, depending on the bioreactor design the appropriate flow rate has to be adjusted. In general, Bjerre et al. as well as Du et al. have shown that cultivation of scaffolds in perfusion bioreactors leads to higher cell numbers and more advanced osteoblastic differentiation [29, 30].

In the present work, two different cell culture techniques were applied to cultivate osteoblastic cells within porous scaffolds of well-defined inner pore structure in order to optimise seeding efficiency, cell proliferation and differentiation on scaffolds intended for bone tissue engineering. A bone marrow stromal cell line (ST-2) was used to investigate cell growth, viability and osteogenic differentiation after 17 days under either static or dynamic cultivation using a perfusion bioreactor system as described previously [24]. Calcium phosphate ceramic scaffolds with varying phase composition (HA, TCP and BCP with

60 wt% HA) and a complex inner network of interconnecting, round-shaped pores were manufactured using an indirect rapid prototyping technique including wax ink-jet printing.

2 Materials and methods

2.1 Scaffold preparation

Computer aided design (CAD) was used to design virtual models of the scaffolds. They were geometrically adapted to the respective culture chamber (Fig. 1) while the pore design was identical in either case.

For static cultivation, cell growth outside the scaffold was avoided by the use of cylindrical scaffolds with a diameter of approximately 14.5 mm and a height of 2.7 mm. In case of the dynamic culture system, a cuboidal shape with $(12 \times 12 \times 10)$ mm³ ensured culture medium flow through instead of around the scaffold.

All scaffolds had a three-dimensional orthogonal network of interpenetrating, round shaped pores with a diameter of approximately 330 μ m, resulting in an open macroporosity of approximately 25 vol%.

Scaffolds were fabricated using an indirect rapid prototyping technique involving wax ink-jet printing as described previously [21]. Briefly, a negative mould of the desired scaffold was designed using a CAD software (SolidWorks 2009) and, subsequently, fabricated by a wax ink-jet printing machine (BT66, Solidscape). During wax ink-jet printing, the model is built layer by layer from molten wax printed on a building platform. Voids are filled with a second wax to support overhangs and hollow spaces. After completion and before the subsequent layer is printed each layer is milled to a predefined thickness. Once the printing process is finished, supporting wax is removed by a solvent and the mould is impregnated with a ceramic slurry. Afterwards, the impregnated mould is dried. During thermal treatment, the remaining wax is burnt out and subsequently the scaffold is sintered.

Hydroxyapatite and tricalcium phosphate powders used in this study were purchased from Merck, Germany.

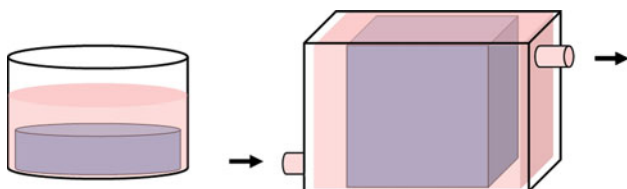


Fig. 1 Sketches of the static (*left*) and dynamic (*right*) cell culture system: scaffolds were designed to geometrically fit the respective culture system

Additionally, a biphasic powder mixture with an HA/TCP weight ratio of 60/40 (HA60) was prepared. The powders were calcined at 900°C for 1 h to decrease slurry viscosity and thus facilitate the impregnation step. A low viscosity aqueous slurry was prepared from each material using a total of 5.5 wt% of organic additives to improve flowability and green part strength. The dried samples were sintered at 1,300°C for 2 h. In order to account for the burn-out of wax and organic additives a dwell time was set at 500°C during heating.

2.2 Cell culture

A bone marrow stromal cell line (ST-2, Deutsche Sammlung für Mikroorganismen und Zellkultur, Germany), isolated from bone marrow of BC8 mice, was used for cell culture experiments. Cells were cultured in RPMI 1640 medium (Gibco, Germany) containing 10 vol% FBS (Sigma-Aldrich, Germany), 1 vol% penicillin/streptomycin (Sigma-Aldrich) and 1 vol% Glutamax (Gibco). During cell culture experiments, the medium was supplemented with 50 μ g/ml ascorbic acid (Sigma-Aldrich), 100 nM dexamethasone (Sigma-Aldrich) and 10 mM β -glycerophosphate (Sigma-Aldrich) for osteogenic stimulation. All scaffolds were seeded with 1 million ST-2 cells. For static cell culture, scaffolds were placed in an incubator (37°C, 5% CO₂) and cultivated for 17 days with change of culture medium every 2–3 days. Furthermore, an optimised perfusion culture bioreactor system [24] was used to incubate scaffolds under dynamic conditions. These scaffolds were pre-cultivated for 3 days under static conditions and were subsequently transferred to an in-house produced perfusion bioreactor system for 14 days. During cultivation an optimised continuous flow-rate of the medium (5 ml/min) was maintained. The medium was pumped in a closed loop with a culture medium reservoir of 150 ml per reactor system, hence no change of medium was necessary.

2.3 Cell distribution

Distribution of cells within the scaffolds was determined by fluorescence microscopy. Samples were washed with phosphate buffered saline (PBS, Biochrom, Germany) and fixed using 3.7 vol% paraformaldehyde (Merck, Germany). Subsequently, the cells were stained using DAPI (Molecular probes, Germany) fluorescence dye and photographed using a fluorescence microscope (Axioplan, Zeiss, Germany). Cell distribution was analysed on top, on bottom and in the middle of the scaffolds. Therefore, scaffolds were embedded in polymeric resin (SpeciFix-40 KIT, Struers, Germany), cut using a band-saw (Proxxon, Germany) and polished (TegraPol-35, Struers) prior to microscopic examination.

2.4 Cell morphology

Cell morphology was characterised via scanning electron microscopy (SEM, Quanta 200, FEI, The Netherlands). For this, cells were fixed in 3 vol% paraformaldehyde, 3 vol% glutaraldehyde (Sigma-Aldrich) and 200 mM sodium cacodylate (Sigma-Aldrich) and dehydrated using a series of graded acetone. Subsequently, samples were CO₂ critical point dried (Parr Instrument Company Moline, USA) and sputtered with gold (sputter coater 108 auto, Cressington, UK).

2.5 Cell proliferation

Cell proliferation was investigated by means of enzyme activity and cell viability. A commercially available lactate dehydrogenase (LDH) quantification kit (TOX7, Sigma-Aldrich) was used to quantify cell proliferation by enzyme activity in cell lysate. Cell viability was measured using the WST-1 assay (Roche, Germany) with a working concentration of 15 µl/ml WST-1 solution in osteogenic medium.

2.6 Cell differentiation

Cell lysates were prepared by immersing the scaffolds in 20 mM TRIS buffered solution (Merck) with 0.1 wt% Triton X-100 (Sigma, Germany), containing 1 mM MgCl₂ (Merck) and 0.1 mM ZnCl₂ (Merck) for 45 min at 37°C and subsequent ultrasonic treatment (VWR, Germany) for 10 min. Alkaline phosphatase (ALP)-activity in the cell lysate was measured colorimetrically using an ALP kit (Sigma-Aldrich) and the specific ALP-activity was calculated referring to the absolute protein concentration of the lysates and incubation time. Therefore, the protein content of the cell lysates was determined using a commercially available kit based on bicinchoninic acid (BCA, Sigma-Aldrich).

Collagen I within the cell lysate was determined using Sirius Red F3BA dye (Chroma, Germany). Samples and collagen I standards were dried, fixed using bouins solution (Sigma-Aldrich) and incubated with Sirius Red dye. Sodium hydroxide was used to dissolve the bound stain. The collagen I content of the samples was measured using an ELISA reader (BMG, Germany) and referred to the determined standard curve.

Furthermore, gene expression of GAPDH, collagen I, osteoprotegerin (OPG), osteocalcin (OC), bone sialoprotein (BSP) and receptor activator of NF-κB ligand (RANKL) were investigated using reverse transcriptase polymerase chain reaction (RT-PCR). RNA was isolated using the MasterPure RNA Purification Kit (Biozym, Germany) following the manufacturer's instructions. Reverse transcription was

performed using unspecific primers (Oligo dT₁₅, Promega, Germany) and the M-MLV RT (Moloney murine-leukaemia-virus reverse transcriptase, 200 U, Promega). For amplification the GoTag Green 2× Master Mix (Promega, Germany) and specific primers were used (sequence, fragment length and annealing temperature are shown in Table 1).

Gel electrophoresis was carried out on a 1.8 wt% agarose gel (LE Agarose, Biozym) with the Sybr Safe (Invitrogen, Germany) gel stain.

2.7 Statistical evaluation

Results are presented as mean value ± standard deviation of four replicates of each sample type. Statistical evaluation was performed by one-way analysis of variance (ANOVA) with a level of statistical significance of $P = 0.05$ (Origin 6.1G, Origin Lab. Corp., USA). All results were normalised to HA (=100%).

3 Results and discussion

3.1 Sample characterisation

Ceramic scaffolds used in this study are shown in Fig. 2. In case of static cell culture scaffolds, pore diameters were 334.9, 328.7 and 320.3 µm in the sintered state for HA, HA60 and TCP scaffolds, respectively. Sintered scaffolds for bioreactor experiments had pore diameter values of 306.7, 326.3 and 308.9 µm. The variation in pore size between the different materials is due to the shrinkage behaviour of the different ceramics, since identically sized moulds were used for all materials. However, variance in pore diameter within one material and scaffold geometry was very low (below 6%).

Due to the layer-by-layer printing process during wax ink-jet printing and the high accuracy of the casting step, the scaffolds had anisotropic surface characteristics. While surfaces within the building plane had no significant roughness, surfaces perpendicular to the building platform were highly textured. This effect has been described previously [25].

3.2 Static cell culture

Fluorescence microscope images of HA scaffolds seeded with ST-2 osteoblastic cells after 48 h are shown in Fig. 3. A homogeneous cell distribution was found throughout the scaffolds. Cells were comparably attached to the top and bottom surfaces as well as within the pore channels. Similar results were found for HA60 and TCP.

Table 1 Sequence, fragment length and annealing temperature of the primers used for PCR

Primer	Sequence (fw = forward, rv = reverse)	Fragment length (bp)	Annealing temperature [°C]
GAPDH	fw: 5' ACCACAGTCCATGCCATCAC 3' rv: 5' TCCACCACCCTGTTGCTGTA 3'	452	48
Collagen I	fw: 5' GAACGGTCCACGATTGCATG 3' rv: 5' GGCATGTTGCTAGGCACGAAG 3'	167	48
OPG	fw: 5' TCCTGGCACCTACCTAAAACAGCA 3' rv: 5' CTACACTCTCGGCATTCACCTTTGG 3'	579	55
OC	fw: 5' AAGCAGGAGGGCAATAAGG 3' rv: 5' CAGAGTTTGGCTTTAGGGC 3'	209	55
BSP	fw: 5' ACCGGCCACGCTACTTTCTTT 3' rv: 5' GACCGCCAGCTCGTTTTC 3'	431	55
RANKL	fw: 5' GCCGAGGAAGGGAGAGAACGAT 3' rv: 5' CGCTCGAAAGTACAGGAACAGA 3'	277	55

Fig. 2 Scaffolds for static (*top*) and perfusion (*bottom*) cell culture experiments fabricated from HA (*left*), HA60 (*middle*) and TCP (*right*) with an interconnecting macroporosity consisting of round shaped pores

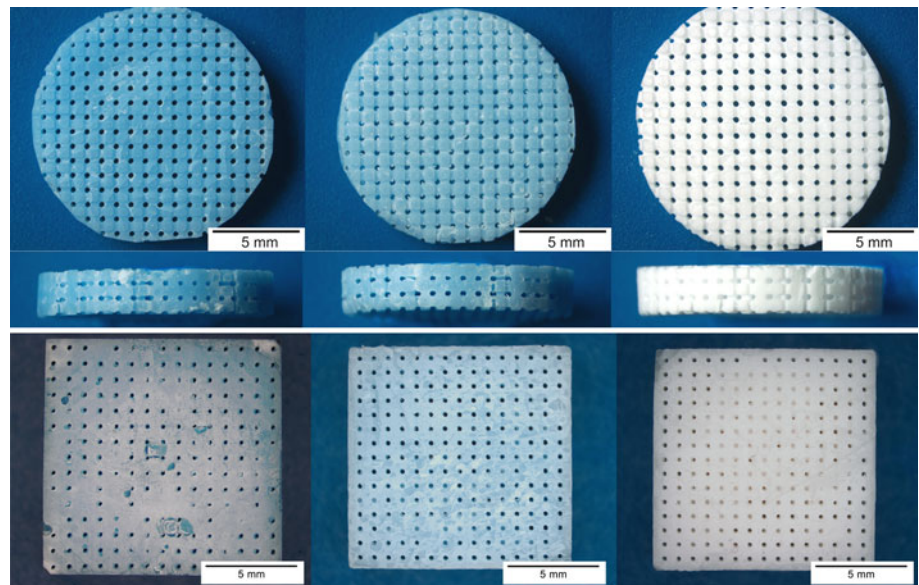
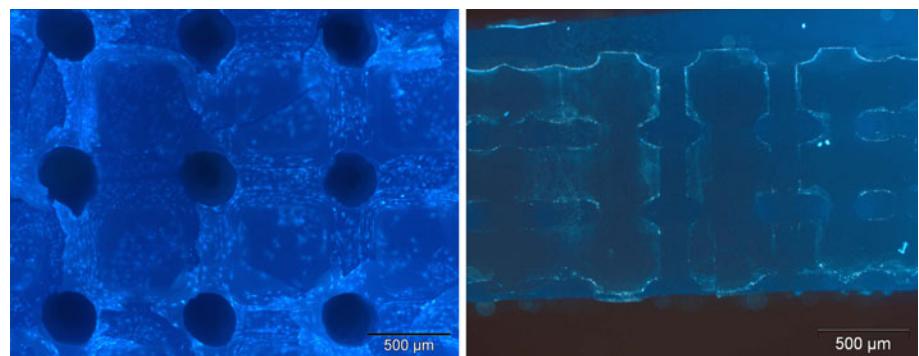


Fig. 3 HA scaffolds seeded with ST-2 cells after 48 h static cultivation (DAPI fluorescent staining). Cells are attached to the scaffolds' outer surface (*left*) as well as within the pore channels (*right*)



SEM micrographs of the top surfaces as well as the inner pore system of scaffolds cultured for 17 days under static conditions are shown in Fig. 4.

All cells on the outer surface of the scaffolds had an osteoblastic cuboidal morphology. Cell membranes showed

blebs and microspikes which indicate high metabolic activities. Within the pores, the anisotropic surface texture resulting from the layer-wise production of the negative moulds was partially covered by cells spanning the grooves in the surface.

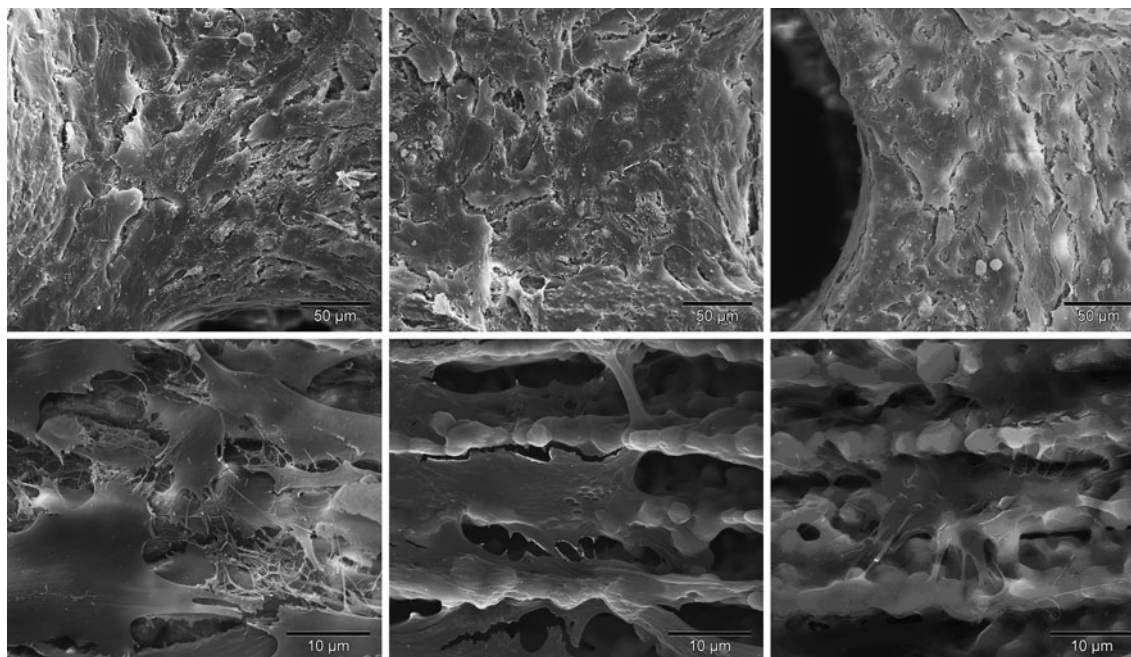


Fig. 4 SEM micrographs of statically cultured ST-2 cells on the scaffold surface (*top*) and within the scaffolds' inner pore system (*bottom*) of HA (*left*), HA60 (*middle*) and TCP (*right*)

However, only few cells were found inside the pore system. This may be attributed to a lack of nutrient or oxygen supply within the pore system of statically cultivated scaffolds, since such supply is limited to diffusion processes. Due to the same limitation, metabolic products as well as degradation products of the scaffold material may accumulate within the pore channels, potentially reaching a level inhibiting cell development. Cell seeding experiments evaluated after 48 h (Fig. 3) had shown a homogeneous cell distribution throughout the whole scaffold. Therefore, cells initially attached in the inner pore system may either have stalled or migrated to the scaffold surfaces. Similar cell distributions within large scaffolds due to diffusion limitations have been described in literature [17, 29–31].

Viability and cell differentiation were investigated after 17 days. The highest cell viability was found in cells grown on HA scaffolds (Fig. 5, left). The viability on TCP (25.9%) was significantly lower than on HA60 (83.6%). LDH-activity revealed no difference between HA and HA60 (100.8%), while the activity found on TCP was also significantly lower (83.9%). Since the concentration of LDH is dependent on the cell number in a linear manner [32] and since all scaffolds had been seeded with the same amount of cells, this result indicates a decreased cell proliferation on TCP.

As the chemical solubility of TCP is much higher than that of HA, there might be a relatively high concentration of Ca^{2+} -ions at the cell/material interface on TCP

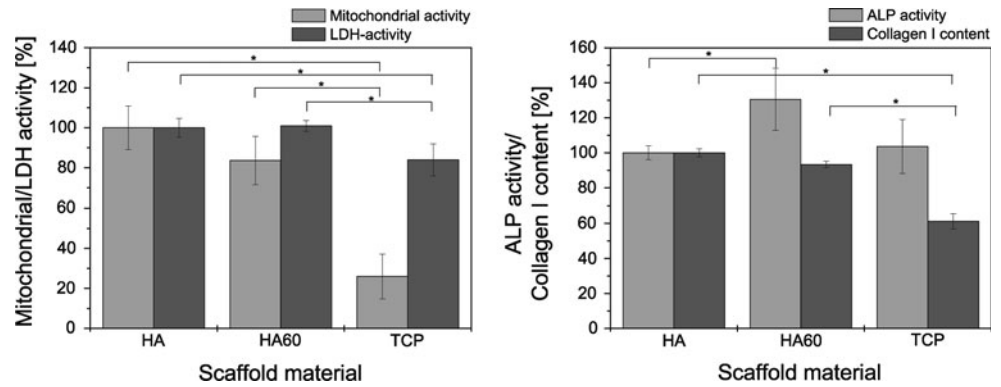
compared to HA. This may be, to a smaller extent, the case on HA60 scaffolds, too. Maeno et al. have shown that the Ca^{2+} -concentration has a distinct influence on osteoblastic cells: viability and osteoblastic differentiation are optimal within small Ca^{2+} -concentration ranges (4–6 mM and 6–8 mM, respectively), while higher concentrations decrease cell viability and inhibit differentiation. Furthermore, cell proliferation was found to be optimal between 2 and 4 mM Ca^{2+} -concentration, being inhibited at higher concentrations [33].

Therefore, the relatively low mitochondrial activity of ST-2 cells on TCP and HA60 samples might be due to locally elevated Ca^{2+} -concentrations. Hence, the drop in viability was less on HA60 because of the lower Ca^{2+} -release compared to TCP.

A significant difference between cells on the three materials was seen by quantitative ALP activity and collagen I content measurement as shown in Fig. 5, right. The highest ALP activity was found in cells cultured on HA60 scaffolds (130.5%), whereas no significant difference between HA and TCP (103.7%) could be detected. Collagen I content, on the contrary, was lowest on TCP (61.2%), compared to HA60 (93.3%) and HA.

The collagen I content indicates a higher extracellular matrix (ECM) production on HA and HA60 scaffolds compared to TCP. Since ECM production is a marker of osteogenic differentiation, this allows the assumption that the osteogenic differentiation of ST-2 cells has reached a similar stage on HA and HA60 scaffolds after 17 days

Fig. 5 Results of cell proliferation and differentiation analysis: mitochondrial- and LDH-activity (*left*) as well as ALP-activity and collagen I content (*right*) of ST-2 cells cultured statically on HA, HA60 and TCP scaffolds over 17 days under osteogenic stimulation ($P > 0.05$)



under static culture conditions, while cells were less differentiated on TCP scaffolds.

RT-PCR revealed that GAPDH, used as control, and collagen I were expressed by cells on all materials (see Table 2; Fig. 6). OPG was found independently of the scaffold material. On the contrary, neither OC, BSP nor RANKL were detected (Table 2).

OPG and collagen I are early markers of the osteogenic differentiation of osteoblast progenitor cells [34, 35], whilst the expression of BSP and OC is characteristic for the late osteoblastic phenotype [35]. In-house analysis of the expression scheme of ST-2 cells under osteogenic stimulation showed that with ongoing differentiation the production of OPG is regulated down at first and afterwards RANKL is expressed. However, no difference in gene expression was found between the cells on the three scaffold materials.

3.3 Perfusion cell culture experiments

Cells attached to the outer surfaces as well as within the inner pore system of CaP-scaffolds after 17 days of cell culture under dynamic conditions are shown in Fig. 7.

The scaffold surfaces were covered with an almost confluent layer of cells exhibiting a cuboidal, osteoblastic phenotype. Moreover, a high density of viable, osteoblast-like cells was found within the inner pore system of the scaffolds, showing a structured cell membrane including

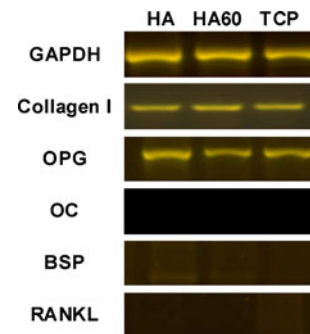


Fig. 6 Results of RT-PCR: gene expression of GAPDH, collagen I, OPG, OC, BSP and RANKL of ST-2 cells cultured on the 3 different scaffolds over 17 days under osteogenic stimulation and static culture conditions

Table 2 Results of RT-PCR: gene expression of GAPDH, collagen I, OPG, OC, BSP and RANKL of ST-2 cells cultured statically on the 3 different scaffolds over 17 days under osteogenic stimulation

	HA	HA60	TCP
GAPDH	+	+	+
Collagen I	+	+	+
OPG	+	+	+
OC	–	–	–
BSP	–	–	–
RANKL	–	–	–

blebs and microspikes which indicate a high metabolic activity. In comparison to the findings on scaffolds cultured under static conditions, the covering of the entire scaffold surface including also the inner pore system can be attributed to the cell culture system. Since in case of dynamic cell culture supply and removal of soluble factors (like nutrients, metabolic or degradation products) is not limited to diffusion processes, an inhibiting environment as assumed to have occurred under static culture conditions could not develop here. Therefore, cells attached within the pore system were able to survive and proliferate. The osteoblastic morphology observed under SEM points to an advanced state of differentiation.

LDH-activity assay revealed comparable results on all three materials, suggesting an almost identical level of cell proliferation independently of the scaffold material (Fig. 8, left). Mitochondrial activity, on the other hand, was significantly increased on HA60 indicating a higher cell viability. As medium perfusion leads to continuous removal of ions, an inhibiting influence of Ca^{2+} resulting from the degradation of TCP as described regarding the static cell culture would not occur in this culture system. Thus, a cell viability comparable to HA could be achieved even on TCP samples. The significant increase of mitochondrial activity

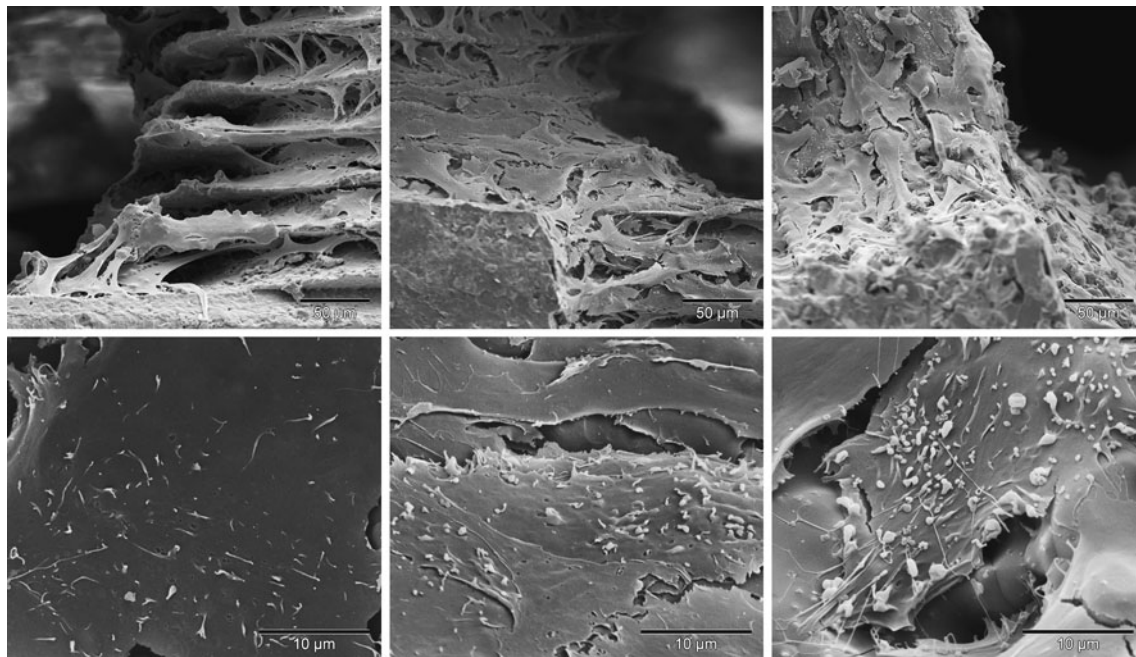
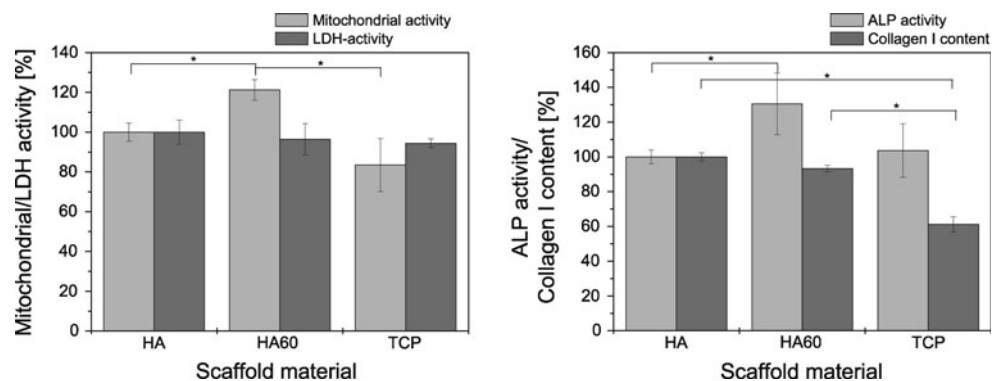


Fig. 7 SEM micrographs of dynamically cultured ST-2 cells within the pore system of HA (left), HA60 (middle) and TCP (right)

Fig. 8 Results of cell proliferation and differentiation analysis: mitochondrial- and LDH-activity (left) as well as ALP-activity and collagen I content (right) of ST-2 cells cultured dynamically on HA, HA60 and TCP scaffolds over 17 days under osteogenic stimulation ($P > 0.05$)



on HA60 might be due to a balance between the HA- and TCP-specific calcium-release on HA60.

Cell differentiation was investigated by means of ALP activity and collagen I content (Fig. 8, right). ALP activity was comparable on HA and HA60 (98.9%), indicating a similar degree of osteoblastic differentiation on these scaffolds. Since the ALP activity was significantly lower on TCP (78.9%), cells were less differentiated on this material. These results are stressed by the quantification of collagen I that revealed the lowest content on TCP (57.0%), while there was no significant difference between HA60 (85.4%) and HA.

Gene expression of osteoblastic marker proteins after 17 days of dynamic cell culture as revealed by RT-PCR is shown in Table 3. Collagen I as well as OC was found on all samples, while no OPG or BSP could be detected. RANKL, being one late marker of the osteoblastic

differentiation, was detected only on HA and HA60 samples but not on TCP (Fig. 9).

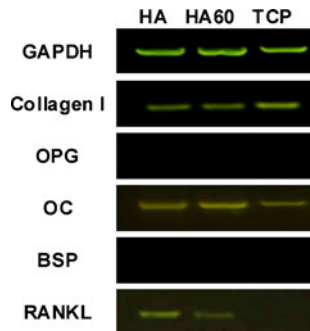
The expression of OC during perfusion culture indicates a more advanced osteogenic differentiation of the cells, since no OC was found in the static culture. This assumption is strengthened by the fact that no OPG but RANKL (on HA and HA60) was found in the perfusion culture. However, the lack of expression of RANKL on TCP indicates a slower differentiation of the ST-2 cells on these samples compared to HA and HA60.

3.4 Comparison of static and dynamic cell culture

Distinct cell growth within the inner pore channels was only found in case of scaffolds cultivated under dynamic conditions, even though the volume of these scaffolds exceeded that of the scaffolds used in the static culture

Table 3 Results of RT-PCR: gene expression of GAPDH, collagen I, OPG, OC, BSP and RANKL of ST-2 cells cultured dynamically on the 3 different scaffolds over 17 days under osteogenic stimulation

	HA	HA60	TCP
GAPDH	+	+	+
Collagen I	+	+	+
OPG	–	–	–
OC	+	+	+
BSP	–	–	–
RANKL	+	+	–

**Fig. 9** Gene expression of GAPDH, collagen I, OPG, OC, BSP and RANKL of ST-2 cells cultured dynamically on the 3 different scaffolds over 17 days under osteogenic stimulation measured using RT-PCR

system by far. HA60 can be regarded as the material most enhancing the osteoblastic cell development, because in both cultivation methods the highest proliferation and cell differentiation was found on the biphasic ceramic, followed by HA and TCP.

With respect to the culture system, an overall more advanced differentiation on scaffolds cultivated under dynamic conditions can be concluded. This is a result of mechanical stimulation through shear stress due to the medium perfusion, the more efficient nutrient supply within the scaffold pore system as well as the constant removal of metabolic waste products and ions released by material degradation. This is in accordance with the findings of Bjerre et al. as well as Du et al. who have shown that cultivation of scaffolds in perfusion bioreactors leads to higher cell numbers and differentiation of osteoblasts [29, 30]. Therefore, the dynamic culture system is more suitable for BTE applications, achieving a homogenous cell distribution with vital cells also throughout the whole pore system and fast differentiation independently of the scaffold material.

4 Summary and conclusion

In this study, a bone marrow stromal cell line (ST-2) in either a static or dynamic cell culture system was used to

fully seed and characterise the in vitro performance of wax ink-jet printing derived calcium phosphate ceramic scaffolds intended to be used as synthetic bone grafts and as scaffolds in bone tissue engineering. The scaffolds were manufactured from HA, TCP and a biphasic mixture with an HA/TCP weight ratio of 60/40 (HA60) and had an interconnecting pore system consisting of perpendicularly arranged round pores of approximately 310–330 μm diameter. Inner and outer scaffold geometry were highly accurate and reproducible, confirming the potential of wax ink-jet printing derived CaP scaffolds for patient-specific bone reconstruction.

It was shown that cells initially attached not only on the scaffold surfaces but also within the pore system, resulting in fully seeded scaffolds. However, after 17 days of cultivation only few cells were found within the inner pore channels of scaffolds cultured under static conditions. On the contrary, a high cell density and homogeneous cell distribution was found even within the inner pores of the scaffolds cultivated in the perfusion bioreactor system. This can be explained by the accumulation of metabolic waste products or shortage of nutrients inside the scaffold that is compensated in the latter case by the perfusion with culture medium. Therefore, the use of perfusion bioreactor systems is the method of choice to cultivate cells within porous scaffolds, allowing to maintain cell growth within the pores of scaffolds of up to $(12 \times 12 \times 10) \text{ mm}^3$ using optimised perfusion parameters. Cell viability and proliferation were similar on HA and HA60, being higher than on TCP in both culture systems. Osteogenic differentiation was found to be more advanced on HA and HA60 scaffolds independently of the cultivation system, which is in accordance to results described in literature [36]. A comparison of the degree of differentiation on statically and dynamically cultured scaffolds revealed an overall more advanced differentiation on scaffolds cultivated under dynamic conditions. This may be due to the better supply of the cells with oxygen and nutrients, the removal of metabolic waste products and ions released through material degradation. Furthermore, optimised medium perfusion through the scaffolds applies stimulating shear stresses. Thus, cell proliferation and differentiation were accelerated by the dynamic cultivation method. These findings are in accordance to the analysis of Bancroft and Jaasma [28, 37], who independently showed that osteoblast cells differentiate faster under dynamic culture conditions.

ST-2 cells on all scaffolds began to differentiate into the osteoblastic lineage, while the highest degree of differentiation was found on HA60, independently of the culture system. With the wax ink-jet printing method for scaffold fabrication from different CaP-ceramics a very exact technique is provided to tailor the scaffolds' geometry to fulfil the requirements of the in vitro cultivation as well as

patient specific needs. As cell proliferation, osteoblastic differentiation of bone precursor cells and particularly persistent cell growth within relatively large scaffolds could be improved by the dynamic culture system, bone tissue engineering employing scaffolds as described here is a promising approach towards the adequate regeneration of individual bone defects.

References

1. Stevens B, Yang Y, Mohandas A, Stucker B, Nguyen K. A review of materials, fabrication methods, and strategies used to enhance bone regeneration in engineered bone tissues. *J Biomed Mater Res B*. 2008;85:573–82.
2. Gazdag AR, Lane JM, Glaser D, Forster RA. Alternatives to autogenous bone graft: efficacy and indications. *J Am Acad Orthop Surg*. 1995;3:1–8.
3. Zipfel GJ, Guiot BH, Fessler RG. Bone grafting. *Neurosurg Focus*. 2003;14:1–8.
4. Itthichaisri C, Wiedmann-Al-Ahmad M, Huebner U, Al-Ahmad A, Schoen R, Schmelzeisen R, Gellrich N. Comparative in vitro study of the proliferation and growth of human osteoblast-like cells on various biomaterials. *J Biomed Mater Res A*. 2007;82:777–87.
5. Hollister SJ. Porous scaffold design for tissue engineering. *Nat Mater*. 2005;4:518–24.
6. Lian JB, Stein GS. Development of the osteoblast phenotype: molecular mechanisms mediating osteoblast growth and differentiation. *Iowa Orthop J*. 1995;15:118–40.
7. Anselme K. Osteoblast adhesion on biomaterials. *Biomaterials*. 2000;21:667–81.
8. Dorozhkin S, Epple M. Biological and medical significance of calcium phosphates. *Angew Chem Int Ed Engl*. 2002;41:3130–46.
9. Woodard JR, Hilldore AJ, Lan SK. The mechanical properties and osteoconductivity of hydroxyapatite bone scaffolds with multi-scale porosity. *Biomaterials*. 2007;28:45–54.
10. Detsch R, Mayr H, Ziegler G. Formation of osteoclast-like cells on HA and TCP ceramics. *Acta Biomater*. 2008;4:139–48.
11. Mayr H, Schlüfter S, Detsch R, Ziegler G. Influence of phase composition on degradation and resorption of biphasic calcium phosphate ceramics. *Key Eng Mat*. 2008;361–363:1043–6.
12. Daculsi G, Laboux O, Malard O, Weiss P. Current state of the art of biphasic calcium phosphate bioceramics. *J Mater Sci Mater Med*. 2003;14:195–200.
13. Raynaud S, Champion E, Lafon JP, Bernache-Assolant D. Calcium phosphate apatites with variable Ca/P atomic ratio III. Mechanical properties and degradation in solution of hot pressed ceramics. *Biomaterials*. 2002;23:1081–9.
14. Davies JE. *Bone engineering*. 1st ed. Toronto: em squared; 2000.
15. Boyan BD, Hummert TW, Dean DD, Schwartz Z. Role of material surfaces in regulating bone and cartilage cell response. *Biomaterials*. 1996;17:137–46.
16. Karageorgiou V, Kaplan D. Porosity of 3D biomaterial scaffolds and osteogenesis. *Biomaterials*. 2005;26:5474–91.
17. Lu JX, Flautre B, Anselme K. Role of interconnections in porous bioceramics on bone recolonization in vitro and in vivo. *J Mater Sci Mater Med*. 1999;10:111–20.
18. Hing KA. Bioceramic bone graft substitutes: influence of porosity and chemistry. *Int J Appl Ceram Technol*. 2005;2:184–99.
19. Habibovic P, de Groot K. Osteoinductive biomaterials—properties and relevance in bone repair. *J Tissue Eng Regen Med*. 2007;1:25–32.
20. Tsang VL, Bhaita SN. Fabrication of three-dimensional tissues. *Adv Biochem Eng/Biotechnol*. 2006;103:189–205.
21. Deisinger U, Hamisch S, Schumacher M, Uhl F, Detsch R, Ziegler G. Fabrication of tailored hydroxyapatite scaffolds: comparison of a direct and an indirect rapid prototyping technique. *Key Eng Mater*. 2008;361–363:915–8.
22. Limpanuphap S, Derby B. Manufacture of biomaterials by a novel printing process. *J Mater Sci Mater Med*. 2002;13:1163–6.
23. Taboas JM, Maddox RD, Krebsbach PH, Hollister SJ. Indirect solid free form fabrication of local and global porous, biomimetic and composite 3D polymer-ceramic scaffolds. *Biomaterials*. 2003;24:181–94.
24. Detsch R, Uhl F, Deisinger U, Ziegler G. 3D-Cultivation of bone marrow stromal cells on hydroxyapatite scaffolds fabricated by dispense-plotting and negative mould technique. *J Mater Sci Mater Med*. 2008;19:1491–6.
25. Wilson CE, de Bruijn JD, van Blitterswijk CA, Verbout AJ, Dhert WJA. Design and fabrication of standardized hydroxyapatite scaffolds with a defined macro-architecture by rapid prototyping for bone-tissue-engineering research. *J Biomed Mater Res A*. 2004;68:123–32.
26. Botchwey EA, Dupree MA, Pollack SR, Levine EM, Laurencin CT. Tissue engineered bone: measurement of nutrient transport in three-dimensional matrices. *J Biomed Mater Res A*. 2003;67:357–67.
27. Chen H, Hu Y. Bioreactors for tissue engineering. *Biotechnol Lett*. 2006;28:1415–23.
28. Bancroft GN, Sikavitsas VI, van den Dolder J, Sheffield TL, Ambrose CG, Jansen JA, Mikos AG. Fluid flow increases mineralized matrix deposition in 3D perfusion culture of marrow stromal osteoblasts in a dose-dependent manner. *Proc Natl Acad Sci USA*. 2002;99:12600–5.
29. Bjerre L, Bungler CE, Kassem M, Mygind T. Flow perfusion culture of human mesenchymal stem cells on silicate-substituted tricalcium phosphate scaffolds. *Biomaterials*. 2008;29:2616–27.
30. Du D, Furukawa K, Ushida T. Oscillatory perfusion seeding and culturing of osteoblast-like cells on porous beta-tricalcium phosphate scaffolds. *J Biomed Mater Res A*. 2008;86:796–803.
31. Malda J, Rouwkema J, Martens DE, Le Comte EP, Kooy FK, Tramper J, van Blitterswijk CA, Riesle J. Oxygen gradients in tissue-engineered PEGT/PBT cartilaginous constructs: measurement and modeling. *Biotechnol Bioeng*. 2004;86:9–18.
32. Allen M, Millett P, Dawes E, Rushton N. Lactate dehydrogenase activity as a rapid and sensitive test for the quantification of cell numbers in vitro. *Clin Mater*. 1994;16:189–94.
33. Maeno S, Niki Y, Matsumoto H. The effect of calcium ion concentration on osteoblast viability, proliferation and differentiation in monolayer and 3D culture. *Biomaterials*. 2005;26:4847–55.
34. Theoleyre S, Wittrant Y, Tat SK. The molecular triad OPG/RANK/RANKL: involvement in the orchestration of pathophysiological bone remodelling. *Cytokine Growth Factor Rev*. 2004;15:457–75.
35. Malaval L, Roche P, Aubin JE. Kinetics of osteoprogenitor proliferation and osteoblast differentiation in vitro. *J Cell Biochem*. 1999;74:616–27.
36. Wang C, Duan Y, Markovic B, Barbara J, Howlett CR, Zhang X, Zreiqat H. Phenotypic expression of bone-related genes in osteoblasts grown on calcium phosphate ceramics with different phase compositions. *Biomaterials*. 2004;25:2507–14.
37. Jaasma MJ, Plunkett NA, O'Brien FJ. Design and validation of a dynamic flow perfusion bioreactor for use with compliant tissue engineering scaffolds. *J Biotech*. 2008;133:490–6.